Supplementary Information

High O_2 Tolerant Metal-based Catalysts for Selective H_2O_2 Reduction by Constructing an Ultra-thin Oxide Passivation Layer

Yaolan Li,[a] Zhenyao Ding,[a] Yifan Zhou,[a] Zhiping Liu,[a] Lihui Huang,[a] Liping Chen,*[a] and Xinjian Feng*[a]

[a] *State Key Laboratory of Bioinspired Interfacial Materials Science, College of Chemistry, Chemical Engineering and Materials Science, Soochow University, Suzhou 215123, P. R. China.*

E-mail: xjfeng@suda.edu.cn; lpchen@suda.edu.cn

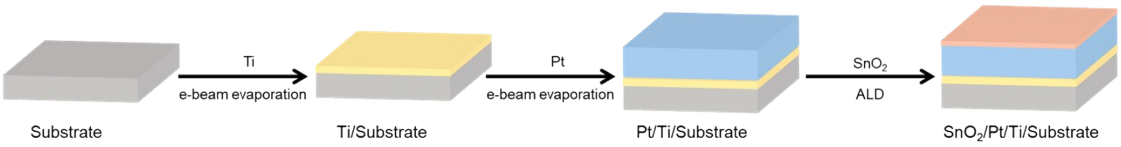

Figure S1. The detail preparation process of Pt/SnO_2.

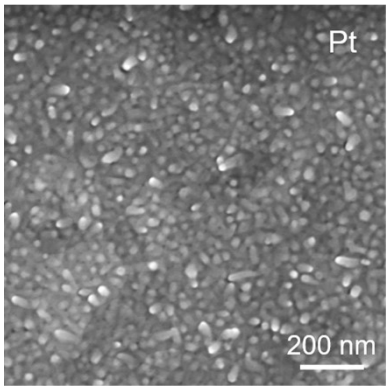

Figure S2. SEM image of the bare Pt catalyst before SnO_2 modification.

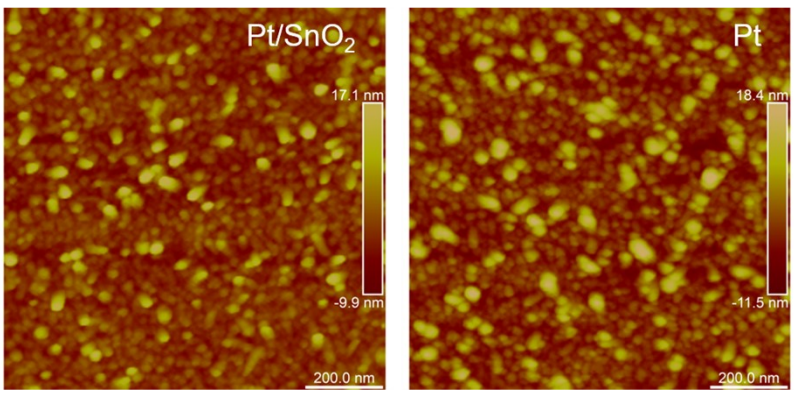

Figure S3. AFM image of the Pt/SnO_2 and bare Pt catalyst.

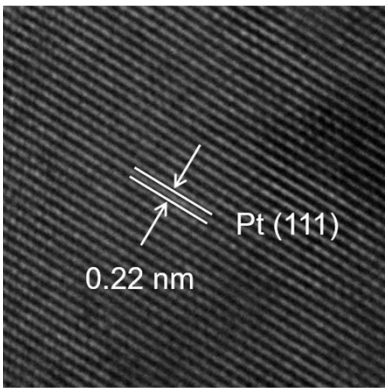

Figure S4. High-resolution TEM image of crystalline Pt. The observed lattice spacing of 0.22 nm corresponded to the (111) facets of Pt.

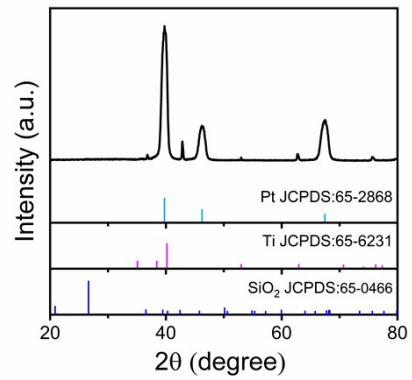

Figure S5. Grazing incident x-ray diffraction (GIXRD) patterns of Pt/SnO_2. Notably, SnO_2 was deposited up to 400 cycles without exhibiting any significant peaks.

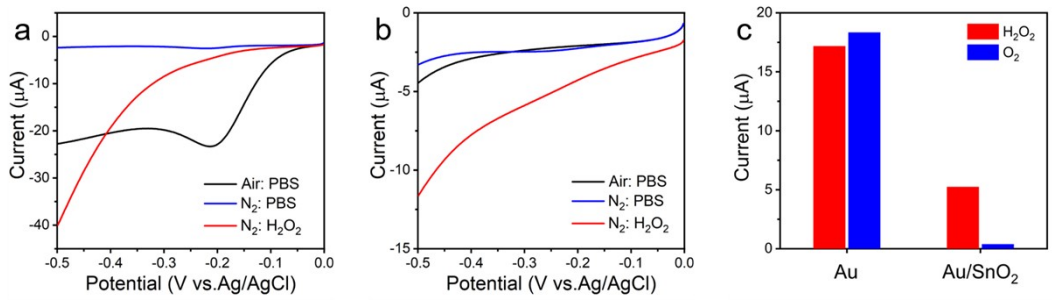

Figure S6. a, b) Oxygen tolerance performance of (a) Au and (b) Au/SnO_2-based electrodes in the H_2O_2 reduction reaction. LSVs curves for Au and Au/SnO_2 are presented in nitrogen-saturated PBS solution (black curves), air-equilibrated PBS solution (blue curves) and nitrogen-saturated H_2O_2 PBS solution (red curves). c) Histogram of the oxygen reduction current (Δi_{O2}, blue columns) and the peroxide reduction current (Δi_{H2O2}, red columns) of Pt/SnO_2 within different cycles of SnO_2 ALD.

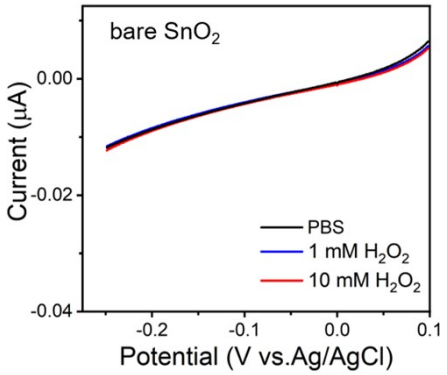

Figure S7. The current response to 1 mM and 10 mM H_2O_2 when SnO_2 deposited on Si substrate directly without Pt.

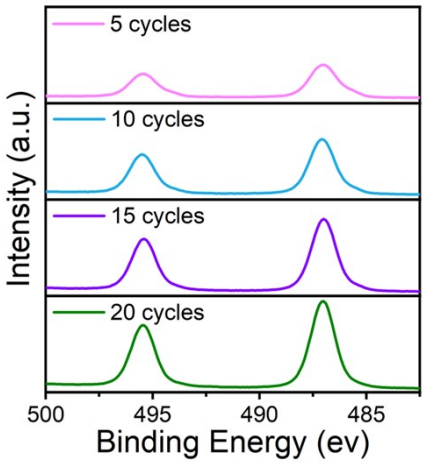

Figure S8. XPS analysis for Sn 3d spectra of SnO_2 for 5, 10, 15 and 20 ALD cycles.

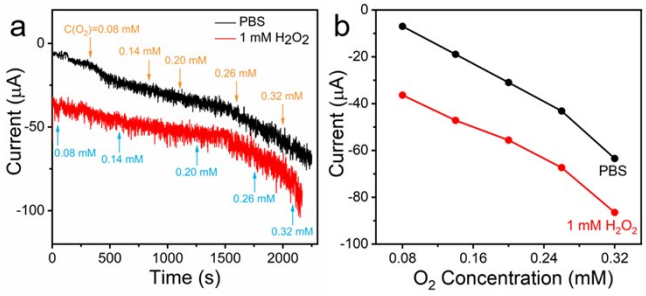

Figure S9. a) Current responses of the Pt based electrode in blank PBS and PBS containing 1×10^{-3} M of H_2O_2 with varying oxygen concentrations. b) The currents of Pt based electrode at certain oxygen levels.

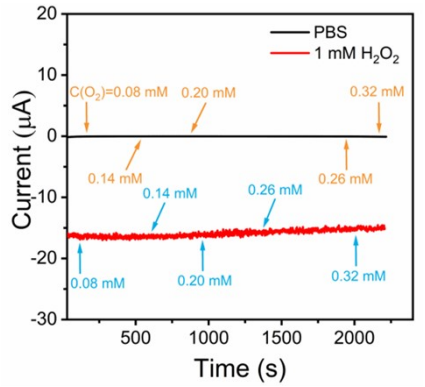

Figure S10. Current responses of the Pt/ SnO_2 based electrode in blank PBS and PBS containing 1×10^{-3} M of H_2O_2 with varying oxygen concentrations.

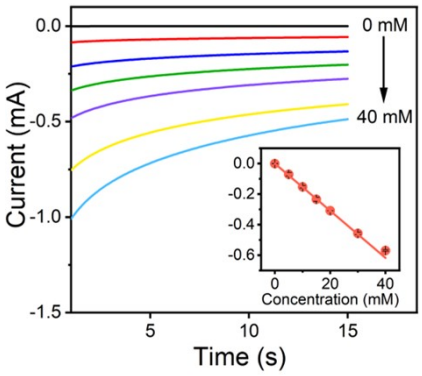

Figure S11. Amperometric responses with different H_2O_2 concentrations ranging from 0 to 40 mM in PBS solution. The inset is the corresponding calibrated curves at 10 s.

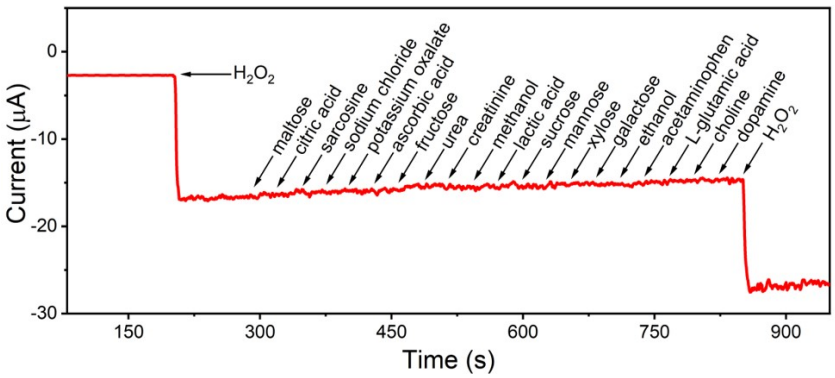

Figure S12. Amperometric responses of the Pt/SnO_2-based electrode upon addition of 1 mM H_2O_2 followed by 1 mM interferents, including maltose, citric acid, sarcosine, sodium chloride, potassium oxalate, ascorbic acid, fructose, urea, creatinine, methanol, lactic acid, sucrose, mannose, xylose, galactose, ethanol, acetaminophen, L-glutamic acid, choline, dopamine.

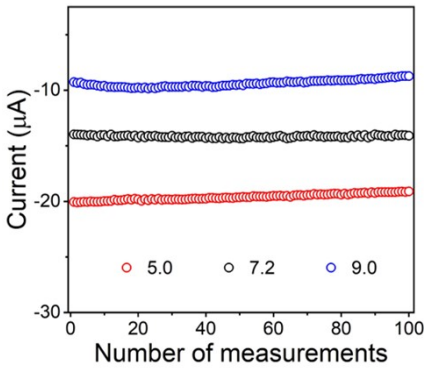

Figure S13. Stability tests of electrolytes with pH values of 5.0, 7.2, and 9.0 for 100 measurements.

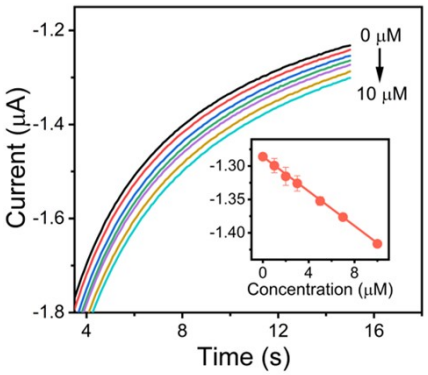

Figure S14. Amperometric responses with low concentration glucose concentrations ranging from 0 to 10 μM in PBS solution.

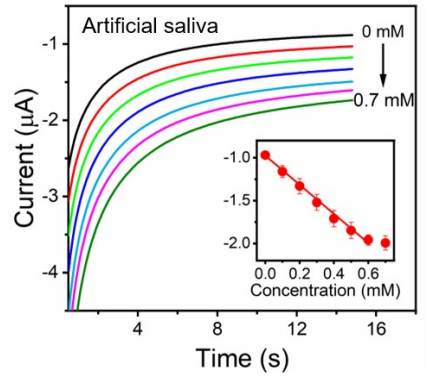

Figure S15. Amperometric responses with different glucose concentrations ranging from 0 to 0.7 mM in undiluted artificial saliva. The inset illustrates the calibration curve at 10 s.

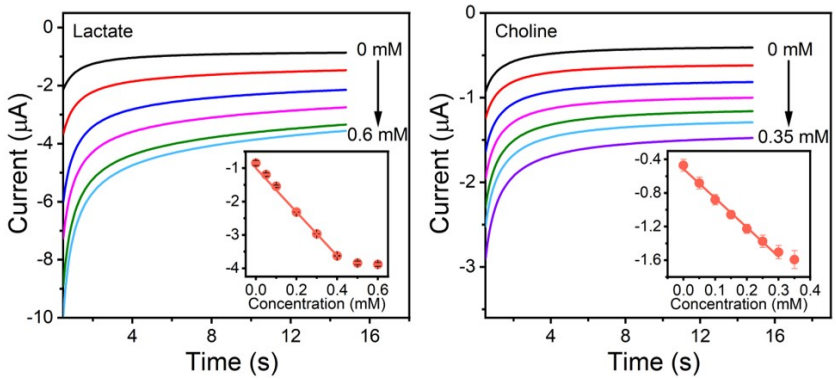

Figure S16. Amperometric responses of Pt/SnO_2-based enzyme electrodes in lactate and choline respectively. Insets show the calibrated curves at 10 s.

Table S1 Comparison of analytical features of the Pt/SnO_2 sensing platform and other sensing platforms for the electrochemical detection of hydrogen peroxide.

Catalysts	$V_{applied}$ vs. Ag/AgCl(V)	Sensitivity ($\mu A \cdot mM^{-1} \cdot cm^{-2}$)	Linear range (μM)	LOD(μM)	Ref.
NGQD@NC@Pd	0	590	Up to 1400	0.02	1
Pt@Co/MoN	-0.25	Not mentioned	0.6-979	0.313	2
AuNFs/(PEI/PAA)/GR/GCE	-0.4	507.5	5-5000	4.5	3
Co_9S_8@CuS	-0.2	411.74	50–14000	6.06	4
A–Co@N/G	-0.3	3428.57	5-5375	0.17	5
Se/P@N-CNBs/CNFs	-0.6	120.3	5-40000	1	6
Pt/SnO_x	-0.05	27.2	0.5-80000	0.5	7
Pt/SnO_2	-0.2	59.2	0.1-40000	0.1	This work

References

1 J. Xi, C. Xie, Y. Zhang, L. Wang, J. Xiao, X. Duan, J. Ren, F. Xiao and S. Wang, *ACS Appl. Mater. Interfaces*, 2016, **8**, 22563–22573.

2 J. Liu, X. Li, L. Cheng, J. Sun, X. Xia, X. Zhang, Y. Song, D. Sun, J. Sun and L. Zhang, *Chem. Commun.*, 2023, **59**, 474–477.

3 L. Zhang, Y. Wang, Y. Wang, M. Guo, Z. Li, X. Jin and H. Du, *Talanta*, 2023, **261**, 124600.

4 C. Zhang, Y. Li, H. Wang, X. Niu, D. Deng, X. Qin, X. Yan, H. He and L. Luo, *Microchem. J.*, 2022, **183**, 108037.

5 J. Li, J. Wu, F. Shi, M. Wang, Z. Zou, Z. Lu, L. Dai and C. M. Li, *Chem. Eng. J.*, 2025, **508**, 160786.

6 W. Zhou, S. Huang and C. Sun, *Int. J. Hydrog. Energy*, 2022, **47**, 14906–14915.

7 Z. Ding, D. Wang, L. Chen, H. Zhou, X. Zhang, X. Feng and L. Jiang, *Adv. Mater. Interfaces*, 2022, **9**, 2102163.